

A simple two-step Riemann solver that separates acoustic waves from contact and shear waves

Mingyu Sun

Corresponding author: sun@fmail.ifs.tohoku.ac.jp

Institute of Fluid Science, Tohoku University, Sendai 980-8577, Japan

Abstract: The Euler equations consist of two acoustic waves ($u \pm c$), contact and shear waves moving at the speed of (u). The acoustic waves are an essential ingredient in compressible flows, but trivial in low Mach number flows. However, most of the upwind schemes treat these waves in the same fashion. In this paper, we propose a method to separate the acoustic waves from the convective waves, resulting in a simple and unique Riemann solver. It is of great advantage for the two-step method to allow different solution-strategies for each step.

Keywords: Approximate Riemann solver, Upwind scheme, Lagrange-Remap, Compressible flows

1 Introduction

The upwind schemes, proven to be able to monotonely capture a discontinuity with the minimum amount of artificial viscosity for the 1-D scalar hyperbolic equation, have gained great acceptance in industrial applications and academic studies[4], especially in problems associated with shock waves. The Euler equations consist of two acoustic waves, contact and shear waves moving at the speed of flow particle. The realization of a upwind discretization for the system of the Euler equations is not simple, since the waves are generally not unidirectional. The Godunov-type approach solves this problem by pursuing an exact or approximate solution to wave interactions, while the flux vector splitting approach decomposes the system such that each subsystem is unidirectional. For multi-dimensional Euler equations, the extension based on the 1D Riemann upwind solvers, which neglects the contribution of shear waves, contains a large amount of empiricism and must therefore remain suspect, although these schemes have been successfully applied to practical problem. Many Godunov-type schemes contain subtle flaws that can cause spurious solutions [2].

On the other hand, the acoustic waves are an essential ingredient in compressible flows, but they even do not explicitly appear in incompressible flows. The upwind treatment for the acoustic waves faces a number of problems when applied to low Mach number flows, such as the loss of accuracy due to numerical diffusion of the order of $O(1/M)$, cancellation in the pressure variable, stiffness of the equations. These facts suggest that the acoustic waves should be treated in a different manner, preferably treated separately from the other waves. However, the common upwind schemes treat all waves in the same fashion.

This work tries to construct an upwind method that solves the acoustic waves and the other waves in two separate steps. The solution to the acoustic waves relies only on the estimation of pressure and velocity at material interface.

2 Basic idea and first order scheme

Consider the one-dimensional system of conservation laws for any fluids,

$$\mathbf{U}_t + \mathbf{F}_x = 0, \tag{1}$$

where \mathbf{U} , \mathbf{F} are vectors of conservative quantities and fluxes. The flux vector can be written as

$$\mathbf{F} = u\mathbf{U} + \mathbf{P}, \quad (2)$$

where $\mathbf{U} = (\rho, \rho u, \rho E)^T$ and $\mathbf{P} = (0, p, pu)^T$. The specific total energy contains the specific internal energy and kinetic energy, $E = e + u^2/2$. For the numerical solution of (1), we shall consider a conservative scheme

$$\Omega_i \mathbf{U}_i^{n+1} = \Omega_i \mathbf{U}_i^n - \Delta t (\mathbf{F}_{i+1/2}^* - \mathbf{F}_{i-1/2}^*), \quad (3)$$

where Δt and Ω_i is the time step and the cell volume respectively. Conservative schemes are different at the way to define flux vector \mathbf{F}^* . In this paper, we consider a two-step method to approximate it. The idea is stimulated by the work of Després et al. [1], in which the authors tried to capture a sharp contact discontinuity using a downwind advection scheme.

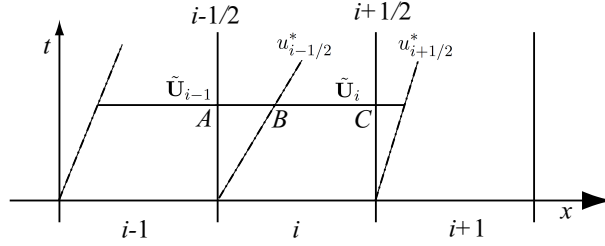


Figure 1: Construction of the two-step Riemann solver

In the first step, we consider a fluid particle occupies cell i bounded by two faces $i + 1/2$ and $i - 1/2$. The conservative quantities of this particle satisfies

$$\tilde{\Omega}_i \tilde{\mathbf{U}}_i = \Omega_i \mathbf{U}_i^n - \Delta t (\mathbf{P}_{i+1/2}^* - \mathbf{P}_{i-1/2}^*), \quad (4)$$

where the tilded variables represent the particle states in the next time step, or the solution in the Lagrangian frame. The volume of the particle evolves, following

$$\tilde{\Omega}_i = \Omega_i + \Delta t (u_{i+1/2}^* - u_{i-1/2}^*).$$

Notice that the flux vector is \mathbf{P} instead of \mathbf{F} . Because of the motion of the particle, it will be advected away from the original Eulerian cell in general, as shown in Fig.1.

In the second step, the conservative quantities in the Eulerian cell i is found by remapping the Lagrangian solution. As shown in Fig.1, they are the sum of two portions, AB and BC . Suppose the Lagrangian solution is piecewise constant, we get

$$\Omega_i \mathbf{U}_i^{n+1} = (u_{i-1/2}^* \Delta t) \tilde{\mathbf{U}}_{i-1} + (\tilde{\Omega}_i - u_{i+1/2}^* \Delta t) \tilde{\mathbf{U}}_i. \quad (5)$$

Substituting (4) into (5), we get

$$\Omega_i \mathbf{U}_i^{n+1} = \Omega_i \mathbf{U}_i^n - \Delta t (\tilde{\mathbf{U}}_i u_{i+1/2}^* + \mathbf{P}_{i+1/2}^* - \tilde{\mathbf{U}}_{i-1} u_{i-1/2}^* - \mathbf{P}_{i-1/2}^*). \quad (6)$$

Compared with (3), the numerical flux of the two-step approach (6) reads,

$$\mathbf{F}^* = \mathbf{U}_{i+1/2}^* u_{i+1/2}^* + \mathbf{P}_{i+1/2}^*, \quad (7)$$

where

$$\mathbf{U}_{i+1/2}^* = \begin{cases} \tilde{\mathbf{U}}_i & \text{for } u_{i+1/2}^* \geq 0, \\ \tilde{\mathbf{U}}_{i+1} & \text{for } u_{i+1/2}^* < 0. \end{cases} \quad (8)$$

The numerical flux relies solely on the estimate of interfacial pressure and velocity, p^* and u^* , which is more or less simpler than most Riemann solver that can resolve a stationary contact. Following the three-wave configuration proposed by Toro et al. [5], and choosing $(u - c)$ and $(u + c)$ as two wave speeds, we obtain

the estimates for pressure and velocity

$$p^* = \frac{I^R p^L + I^L p^R}{I^L + I^R} + \frac{I^L I^R}{I^L + I^R} (u^L - u^R) \quad (9)$$

$$u^* = \frac{I^L u^L + I^R u^R}{I^L + I^R} + \frac{1}{I^L + I^R} (p^L - p^R) \quad (10)$$

where $I^L = \rho^L c^L$, and $I^R = \rho^R c^R$ are acoustic impedances on two sides.

Remarks on acoustic waves in the Lagrange step The Lagrange step updates the conservative quantities of a moving particle by (4). The equations physically reflect: (a) the mass of the particle remains constant, (b) the momentum and the energy evolve with the pressure and velocity at the boundary of the particle. The flux vector \mathbf{P} contains only two scalar quantity, pressure p and velocity u . Under the isentropic assumption, the momentum and the energy equation in the Lagrange frame can be expressed as, respectively

$$\rho \frac{Du}{Dt} + p_x = 0, \quad (11)$$

and

$$\frac{1}{\rho c^2} \frac{Dp}{Dt} + u_x = 0, \quad (12)$$

where isentropic sound speed $c^2 = (\frac{Dp}{D\rho})_s$. The Jacobian matrix of the system is

$$\begin{vmatrix} 0 & \rho c^2 \\ 1/\rho & 0 \end{vmatrix},$$

with eigenvalues of $(-c, c)$. It is clear that only acoustic waves are handled in this step.

3 Second-order extension

3.1 The Lagrange step

The second order accuracy of the Lagrange step in space is achieved by following the MUSCL method. The pressure and velocity at interfaces are interpolated from the cell center,

$$\mathbf{M}_{i+1/2} = \mathbf{M}_i + \Phi_i^L [(\nabla \mathbf{M})_i \frac{\Delta x}{2} + (\mathbf{M}_t)_i \frac{\Delta t}{2}] \quad (13)$$

where $\mathbf{M} = (p, u)^T$, and the MINMOD slope limiter is used for limiter function Φ_i^L . Time derivative, \mathbf{M}_t , is included to achieve second order accuracy in time, which is calculated from (11) and (12) using the values and gradients at the last time step.

3.2 The remap step

The first order remap uses the piecewise constant state to represent the solution in the Lagrangian frame, as shown in Fig. 2a. The second order accuracy can be achieved using the piecewise linear reconstruction of the states (Fig. 2b). This problem is similar to the construction of a limiter in the MUSCL approach for hyperbolic equations, but not the same.

For the sake of clarity, we hereafter assume a constant positive velocity $u > 0$. Instead of using (8), the conservative states are interpolated from the upstream cell,

$$\mathbf{U}_{i+1/2}^* = \tilde{\mathbf{U}}_i + \Phi_i^R (\nabla \tilde{\mathbf{U}})_i \Delta_i^+, \quad (14)$$

where Φ_i^R is the slope limiter that modifies the gradient $(\nabla \tilde{\mathbf{U}})_i$, to be defined later, and

$$\Delta_i^+ = \tilde{x}_{i+} - \tilde{x}_i = (x_{i+1/2} + u\Delta t/2) - (x_i + u\Delta t) = (x_{i+1/2} - x_i) - u\Delta t/2. \quad (15)$$

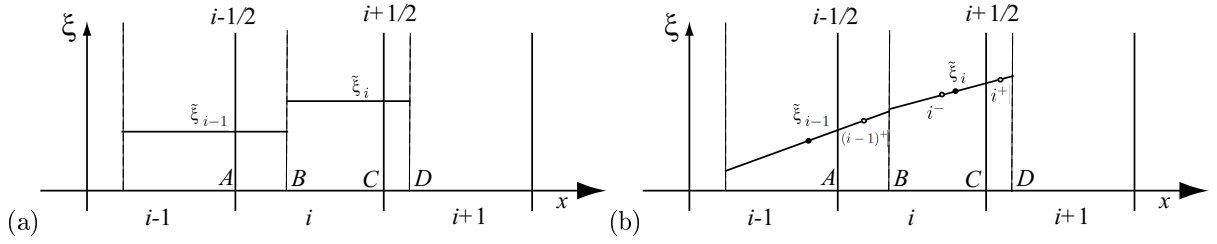


Figure 2: The remap step: (a) first order remap; (b) second-order remap

Notice that the interpolated value is located not at the cell interface as commonly followed in MUSCL-type schemes, but at the center between grid and particle interfaces, as denoted by empty circles in Fig. 2b. The values at this central point represents the average state of the portion, CD , to second order accuracy. One may also interpolate other set of variables, e.g. $\mathbf{R} = (\rho, u, e)$, and then the conservative states are evaluated from interpolated variables,

$$\mathbf{U}_{i+1/2}^* = \tilde{\mathbf{U}}(\mathbf{R}_i + \Phi_i^R(\nabla \tilde{\mathbf{R}})_i \Delta_i^+). \quad (16)$$

It is more convenient to preserve positivity of internal energy in the remap step. The use of non-conservative state variables neither degenerates the order of accuracy, nor violates the conservation laws since the overall conservation is preserved by following (3).

We shall construct the slope limiter Φ_i^R such that the second-order remap step will not create numerical oscillations. The remap step is generally expressed as

$$\Omega_i \xi_i = \Omega_{AB} \tilde{\xi}_{(i-1)^+} + \Omega_{BC} \tilde{\xi}_{i^-}, \quad (17)$$

which represents a volume-weighted average of two central values in portions AB and BC , as shown in Fig. 2b. Function ξ represents a variable to be interpolated. The downstream value is interpolated by

$$\tilde{\xi}_{i^+} = \tilde{\xi}_i + \Phi_i^R(\nabla \tilde{\xi})_i \Delta_i^+. \quad (18)$$

The upstream value, representing the average state of the remaining quantities between BC in the Eulerian cell i , is interpolated similarly,

$$\tilde{\xi}_{i^-} = \tilde{\xi}_i + \Phi_i^R(\nabla \tilde{\xi})_i \Delta_i^-, \quad (19)$$

where

$$\Delta_i^- = \tilde{x}_{i^-} - \tilde{x}_i = (x_i + u\Delta t/2) - (x_i + u\Delta t) = -u\Delta t/2. \quad (20)$$

The slope limiter Φ^R is defined such that the remap step does not introduce any new extrema. The following TVD (Total Variation Diminishing) condition,

$$\min(\tilde{\xi}_{i-1}, \tilde{\xi}_i) \leq \xi_i \leq \max(\tilde{\xi}_{i-1}, \tilde{\xi}_i), \quad (21)$$

should be satisfied. Since $|\Delta_i^+|, |\Delta_i^-| \leq \Delta x/2$ for $u\Delta t/\Delta x \leq 1$, it is sufficient to fulfill (21), if two interpolated values at cell boundaries satisfy, for all i ,

$$\min(\tilde{\xi}_{i-1}, \tilde{\xi}_i) \leq \tilde{\xi}_{i-1/2} \leq \max(\tilde{\xi}_{i-1}, \tilde{\xi}_i), \quad (22)$$

$$\min(\tilde{\xi}_i, \tilde{\xi}_{i+1}) \leq \tilde{\xi}_{i+1/2} \leq \max(\tilde{\xi}_i, \tilde{\xi}_{i+1}), \quad (23)$$

where the middle values are interpolated from $\tilde{\xi}_{i-1/2} - \tilde{\xi}_i = -(\nabla \tilde{\xi})_i \Delta x/2$, and $\tilde{\xi}_{i+1/2} - \tilde{\xi}_i = (\nabla \tilde{\xi})_i \Delta x/2$.

We devise the following MINMOD slope limiter,

$$\Phi_i^R = \begin{cases} 0 & r^+ \leq 0 \vee r^- \leq 0, \\ \min(1, r^+, r^-) & \text{otherwise,} \end{cases} \quad (24)$$

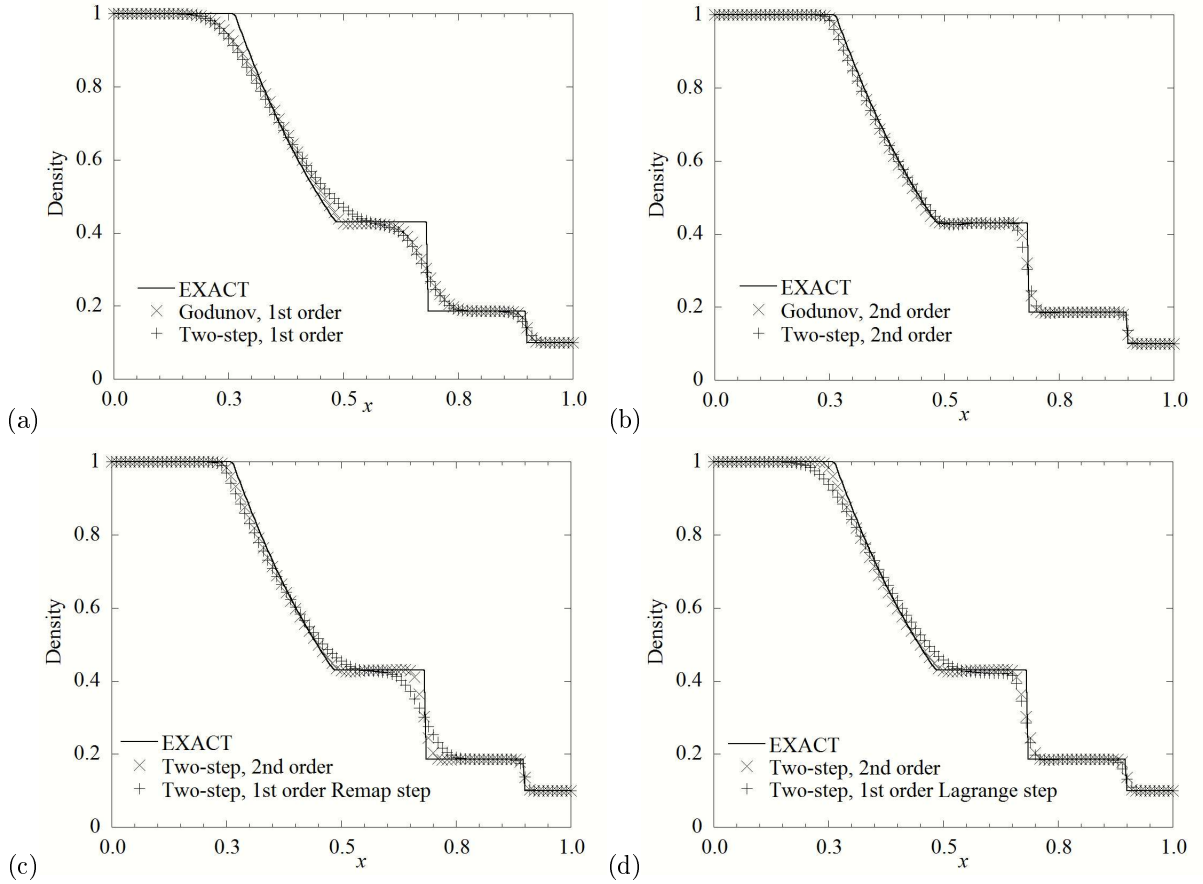


Figure 3: 1D shock tube problem

where

$$r^- = \frac{\tilde{\xi}_{i-1} - \tilde{\xi}_i}{\tilde{\xi}_{i-1/2} - \tilde{\xi}_i}, r^+ = \frac{\tilde{\xi}_{i+1} - \tilde{\xi}_i}{\tilde{\xi}_{i+1/2} - \tilde{\xi}_i}. \quad (25)$$

One may show (24) satisfies (22) and (23), after a few algebraic manipulations. No attempt has been made to devise any anti-diffuse limiter, which violates the second law of the thermodynamics although it may resolve a sharper contact discontinuity numerically.

4 Numerical results and discussion

The ideal gas equation of state is used in numerical simulation. The CFL number is taken as 0.8 for 1D tests, and 0.45 for 2D tests. The results of the well-known Sod shock tube are shown in Fig 3. The results of the first-order and second-order schemes are compared with the Godunov schemes using the exact Riemann solver in Figs. 3ab. The second-order Godunov scheme is constructed based on the MUSCL-Hancock method. It is seen that the two-step solvers resolve the shock, contact and expansion waves as well as its Godunov counterpart. The first order version behaves more diffusive at the location where the initial discontinuity breaks. It is just the location where a upwind scheme may create an expansion shock.

The present two-step approach allows us to adopt different numerical schemes for the acoustic waves and the contact discontinuity. For instance, one may construct a two-step scheme combining the second-order Lagrange step with the first-order Remap, and vice versa. The results of these two partially second-order schemes are plotted in Figs. 3cd, together with the fully second-order scheme. With the first-order remap, the contact wave is widen similarly to the first order scheme (Fig. 3a), while other waves are resolved as well as the second-order scheme. If the first-order Lagrange scheme coupled with the second-order remap, the leading front of left traveling expansion waves is smeared, as seen in the first order scheme 3a, but the

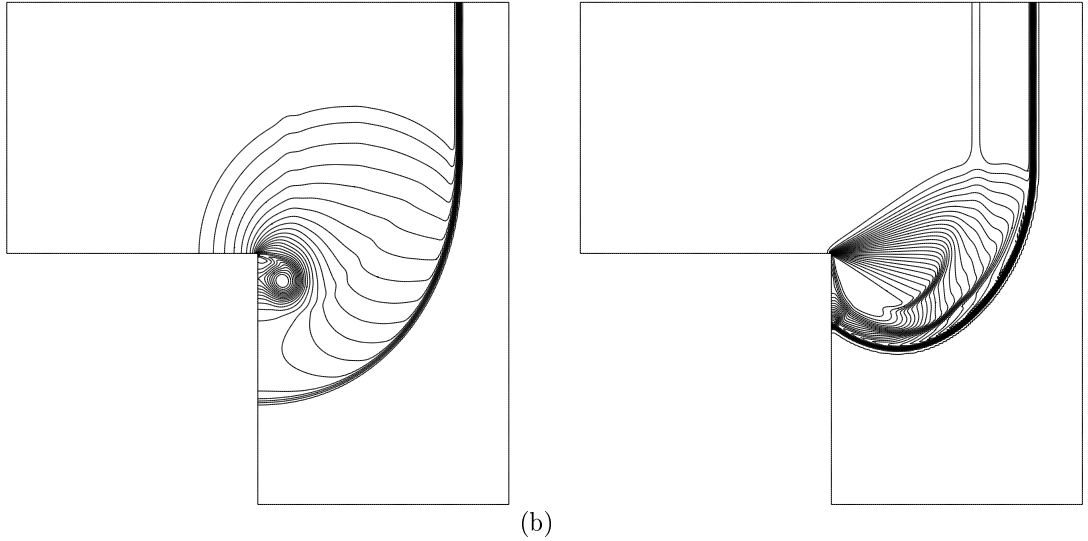


Figure 4: Unsteady shock wave diffraction over a 90° corner, isopycnics: (a) $M_s = 1.5$, (b) $M_s = 8$.

contact hardly changes. As a 2D illustration, shock wave diffraction over a 90° corner is conducted, as done in [3]. The geometry consists of three 1×1 squares, and each is divided to 128×128 uniform cells. A shock wave is initially at 0.5 to the left of the corner point. The results are shown in Fig. 4, for a weak and a strong shock wave. The results are reasonably good.

5 Concluding remarks

We proposed a two-step approach that separate the acoustic waves from the other waves. The resulting Riemann solver of the two-step approach solely relies on the estimate of interfacial pressure and velocity. Numerical tests confirm that one may use different schemes to control artificial viscosity for each of them. This suggest that it is possible to adopt different solution-strategies, say, an implicit method only for the acoustic waves in low Mach number flow regime, which are under development. Although the 1D estimates in the direction normal to the grid interface has been followed for multi-dimension extension in the present work, the approach sheds a new light on the construction of a fully multidimensional Riemann solver.

References

- [1] Després B, Lagoutière F, Contact discontinuity capturing schemes for linear advection and compressible gas dynamics, *J of Scientific Computing*, **16** (2001) 479-524
- [2] Quirk JJ, A contribution to the great Riemann solver debate, *Intl. J. for Numer. Methods in Fluids*, **18**, 555, (1994)
- [3] Sun M, Takayama K, Conservative smoothing on an adaptive quadrilateral grid, *J. Comput. Phys*, **150**, 143, (1999)
- [4] Toro E.F., *Riemann Solvers and Numerical Methods for Fluid Dynamics: A Practical Introduction*, Springer; 2nd edition (1999)
- [5] Toro EF, Spruce M, Speares W, Restoration of the contact surface in the HLL-Riemann solver, *Shock Waves*, **4**, 25, (1994)